iScience

CellPress
OPEN ACCESS

Article

Glioblastoma behavior study under different frequency electromagnetic field

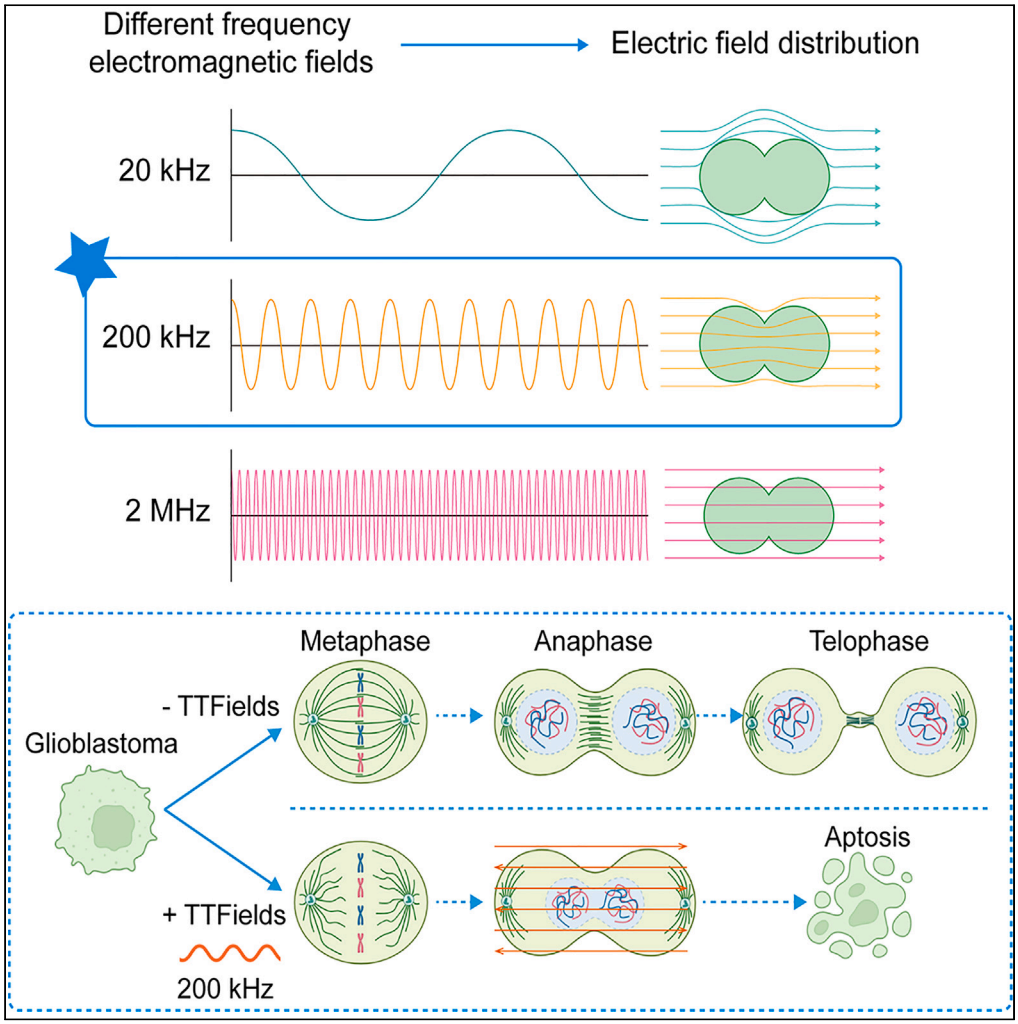

Xiao-Wei Xiang, Hao-Tian Liu, Xiao-Nan Tao, ..., Hui Zhao, Yan-Jun Liu, Ke-Fu Liu

hui_zhao@fudan.edu.cn (H.Z.)
yanjun_liu@fudan.edu.cn (Y.-J.L.)
kfliu@fudan.edu.cn (K.-F.L.)

Highlights

Study aims to understand biophysical principles of TTFields

Simulation predicts increased cleavage furrow region, explaining TTFields' anti-proliferative effects

Frequency and field strength determine TTFields' impact on glioma cell proliferation and migration

Xiang et al., iScience *26*, 108575
December 15, 2023
https://doi.org/10.1016/j.isci.2023.108575

iScience

CellPress
OPEN ACCESS

Article

Glioblastoma behavior study under different frequency electromagnetic field

Xiao-Wei Xiang,[1,5] Hao-Tian Liu,[1,5] Xiao-Nan Tao,[2,5] Yu-Lian Zeng,[3] Jing Liu,[2] Chen Wang,[4] Sai-Xi Yu,[4] Hui Zhao,[2,*] Yan-Jun Liu,[4,*] and Ke-Fu Liu[2,6,*]

SUMMARY

The tumor-treating fields (TTFields) technology has revolutionized the management of recurrent and newly diagnosed glioblastoma (GBM) cases. To ameliorate this treatment modality for GBM and other oncological conditions, it is necessary to understand the biophysical principles of TTFields better. In this study, we further analyzed the mechanism of the electromagnetic exposure with varying frequencies and electric field strengths on cells in mitosis, specifically in telophase. In reference to previous studies, an intuitive finite element model of the mitotic cell was built for electromagnetic simulations, predicting a local increase in the cleavage furrow region, which may help explain TTFields' anti-proliferative effects. Cell experiments confirmed that the reduction in proliferation and migration of glioma cell by TTFields was in a frequency- and field-strength-dependent manner. This work provides unique insights into the selection of frequencies in the anti-proliferative effect of TTFields on tumors, which could improve the application of TTFields.

INTRODUCTION

The conventional approaches toward cancer treatment have undergone a significant transformation over the past two decades, as a result of advancements in our comprehension of tumor progression and resistance to traditional therapies.[1] Brain tumors are usually treated with surgical removal, radiation therapy, and chemotherapy. However, these treatment options come with certain limitations. They may not be highly effective in specific cases, can lead to potential side effects, and might result in the development of resistance. Additionally, their lack of specificity and the influence of tumor heterogeneity on treatment response further contribute to their limitations. Furthermore, the prognosis of gliomas is often poor due to the absence of drug delivery systems that can specifically target brain tumors and overcome the challenges posed by the blood-brain barrier (BBB) and the blood-brain tumor barrier (BBTB).[2]Tumor-treating fields (TTFields) therapy is a well-acknowledged modality of anti-cancer therapy, which uses low-strength intermediate-frequency (IF) alternating current (AC) electric fields. This therapy offers several advantages, including its non-invasive nature and its ability to specifically target localized tumor sites without causing systemic toxicity. Clinically, a randomized trial (EF-14; NCT00916409) demonstrated that patients receiving TTFields therapy alongside standard-of-care treatment experienced significantly prolonged overall survival compared with those receiving standard-of-care treatment alone. The US FDA has approved a treatment known commercially as Optune (Novocure) for the management of newly diagnosed and recurrent glioblastoma (GBM) using extracranial implementation.[3] Clinical studies of TTFields therapy have also been conducted in six other oncology indications, including two randomized, pivotal phase 3 studies in glioblastoma. TTFields therapy has been the subject of clinical studies in six oncology indications, including two pivotal phase 3 studies in glioblastoma.[4] Recently, an implantable ultrasonic-powered TTF device has also been developed by further transferring the stimulation device extracranially to the intracranial level.[5] These devices both verified a relatively high inhibition rate of tumor cell proliferation by this method of TTFields in both *in vitro* and *in vivo* experiments. Although various clinical trials have explored different parameter settings, further research is needed to identify the most effective and efficient treatment protocols tailored to specific tumor types and stages.

Previous studies have focused on the effects of TTFields on the mitosis and cytokinesis.[6] At the cellular level, it has been hypothesized that proteins with significant dipole moments, such as tubulin dimers, may align themselves in response to the electric field generated by TTF. This alignment could potentially disrupt the integrity of the mitotic spindle and interfere with the normal progression of mitosis.[7] Additionally, it was proposed that during the telophase, the electric fields become significantly heterogeneous at the mitotic furrow, thereby subjecting

[1]Academy for engineering & technology, Fudan University, Shanghai 200433, China
[2]School of information science and technology, Fudan University, Shanghai 200433, China
[3]Department of Anesthesiology, Ruijin Hospital, Shanghai Jiao Tong University School of Medicine, Shanghai 200020, China
[4]Shanghai Xuhui Central Hospital, Zhongshan-Xuhui Hospital, Shanghai Key Laboratory of Medical Epigenetics, Shanghai Stomatological Hospital, Institutes of Biomedical Sciences, Fudan University, Shanghai 200032, China
[5]These authors contributed equally
[6]Lead contact
*Correspondence: hui_zhao@fudan.edu.cn (H.Z.), yanjun_liu@fudan.edu.cn (Y.-J.L.), kfliu@fudan.edu.cn (K.-F.L.)
https://doi.org/10.1016/j.isci.2023.108575

biomolecules in the furrow region to dielectrophoretic forces and impairing the process of cell division.[8] However, the biophysical mechanisms of TTFields on mitotic cells are not fully understood, and more studies in electrical parameters such as frequency and field strength selection are needed to support and optimize the application of TTFields in the treatment of GBM and other tumors.

In this study, we used different modeling approaches to precisely assess the effects of different frequencies and electric field strength of TTFields on cells and validated the modeling results in cell experiments. We revealed the frequency dependence and field strength dependence of the TTFields' effect during mitosis. Furthermore, we investigated the effect of TTFields on cell migration, and the trend was consistent with mitosis. Our computational and experimental data provide unique insights into the effect of TTFields on mitotic cells. The proposed model helps to improve the efficiency of TTFields in treating tumors by finding the optimal TTFields parameters.

RESULTS

Disruption and field enhancement during the cell division phase

The mechanism of frequency selection for tumor-treating fields (TTFields) applied in repressing tumor growth is currently unclear, making it difficult to further optimize treatment techniques and applications (Figure 1A). To address this knowledge gap, we conducted simulations to optimize the frequency of the electric field, ranging from 20 kHz to 2 MHz, enabling us to gain valuable insights into the behavior of the electric field at different frequencies (Figures S1A and S1B). Based on the simulation results, we observed a consistent increase in the electric field intensity at regions A and B on both the plasma membrane and nuclear membrane as the frequency ranged from 2 kHz to 200 kHz. This finding suggests that these frequencies have a specific influence on the electric field near the cleavage furrow, which is crucial for cell division. Moreover, our simulations revealed a notable trend as the frequency of the electric field increased from 200 kHz to 2 MHz. Specifically, the nonuniformity near the furrow decreased, indicating a more uniform distribution of the electric field. Furthermore, the overall field intensity throughout the cell increased with higher frequencies (Figure S1C). These findings suggest that higher frequencies lead to a more balanced and potent electric field within the cell. To further investigate these effects for four different cell-cycle stages, we performed electromagnetic simulations at a fixed field intensity of 1 V/cm and varying frequencies of the alternating current (AC) electric field (Figure 1B). For a cell in metaphase, this result demonstrated that the electric field lines were mainly distributed in the medium around the cells when a low-frequency (LF) (20 kHz) alternating electric field is applied. As the frequency increased to intermediate frequency (IF) (200 kHz) and radio frequency (RF) (2 MHz), the electric field lines can penetrate into the cell cytoplasm and cause an increase in the intracellular electric field strength. This phenomenon can be explained by a known mechanism: the cell membrane functions as an insulator at low-frequency (LF) ranges, due to its high electrical resistance relative to the external medium and the intracellular fluid.[9] Meanwhile, at higher frequency regimes starting from approximately 200 kHz, the capacitive properties of the membrane provide a conductive pathway for displacement currents, leading to a reduction in its resistance. However, electromagnetic simulations of the field distribution demonstrated an enhanced intensity of the electric field at frequencies around 200 kHz in the cleavage furrow region for cell in telophase. Furthermore, we quantified the electric field distribution along the central axis of the cell to study the effects caused by electromagnetic fields at the cellular level (Figure 1C). It was noted that the electric field strength in the region of the cleavage furrow in cell membrane and nuclear membrane exceeded the value of the surrounding medium as the progression of cell mitosis. Specifically, during the telophase stage 3 compared with metaphase, we observed a significant 246% increase in electric field strength near the cell membrane invagination for the 200 kHz frequency, reaching up to 4.4 V/cm. This increase was likewise accompanied by a 6-fold rise in electric field strength near the cell nuclear membrane invagination. In contrast, when comparing the 20 kHz and 2 MHz frequencies with the 200 kHz frequency, we observed different trends in the electric field strength near the cell membrane invagination. The 20 kHz frequency exhibited a decrease of 32%, whereas the 2 MHz frequency demonstrated a 3-fold increase (198% higher).

To further investigate the electric field distribution in the cellular level at different electric field strengths, we performed electromagnetic simulations at cellular level with the same frequency alternating current electric field (200 kHz) (Figure S1D). At the same cell mitosis phase, as the external electric field strength increased, the average electric field strength inside the cell also increased. Moreover, as cell mitosis enter telophase, the electric field strength in the cleavage furrow region increased, especially in this region during late telophase compared with metaphase, where the electric field strength increases 4-fold (Figure S1E). Berkelmann et al. indicated that TTFields showed the same trend in power absorption density in cleavage furrow region.[10] Taken together, these simulation results demonstrated that IF currents are able to flow through the cell for the capacitive properties of the membrane, increasing the electric field strength inside the cell, while retaining the resistance to allow significant energy absorption and stronger electric field force in the cleavage furrow region during mitosis. Moreover, this electric field strength of cleavage furrow becomes larger as the region becomes larger during telophase. Stronger electric field forces will have a greater effect on intracellular proteins, such as tubulin dimers, causing the cell mitosis process to be inhibited.

Effect of TTFields on cell proliferation inhibition

Our simulation results have revealed that the electric field distortion is most prominent in the region of the cleavage furrow, which plays a crucial role in cell division. Building upon this observation, we investigated the potential impact of electric fields of different frequencies on cell division. The electric fields of different frequencies may tend to interact with proteins possessing high dipole moments, including the heterotrimeric septin protein complex, which plays a crucial role in positioning the cytokinetic cleavage furrow.[11,12] To verify whether cells exhibit maximal destructive cell proliferation when exposed to specific frequencies of electric fields, we stimulated GBM cell line (U87-MG) through the three frequencies used in previously simulations (Figure 2A). The time-lapse results on dividing cells demonstrated that continuous electrical stimulation at these three frequencies affects the cell division process, especially IF stimulation caused cell membrane blebbing and disruption of the mitotic spindle during telophase (yellow arrow), resulting in cells that do not divide into two cells properly. We

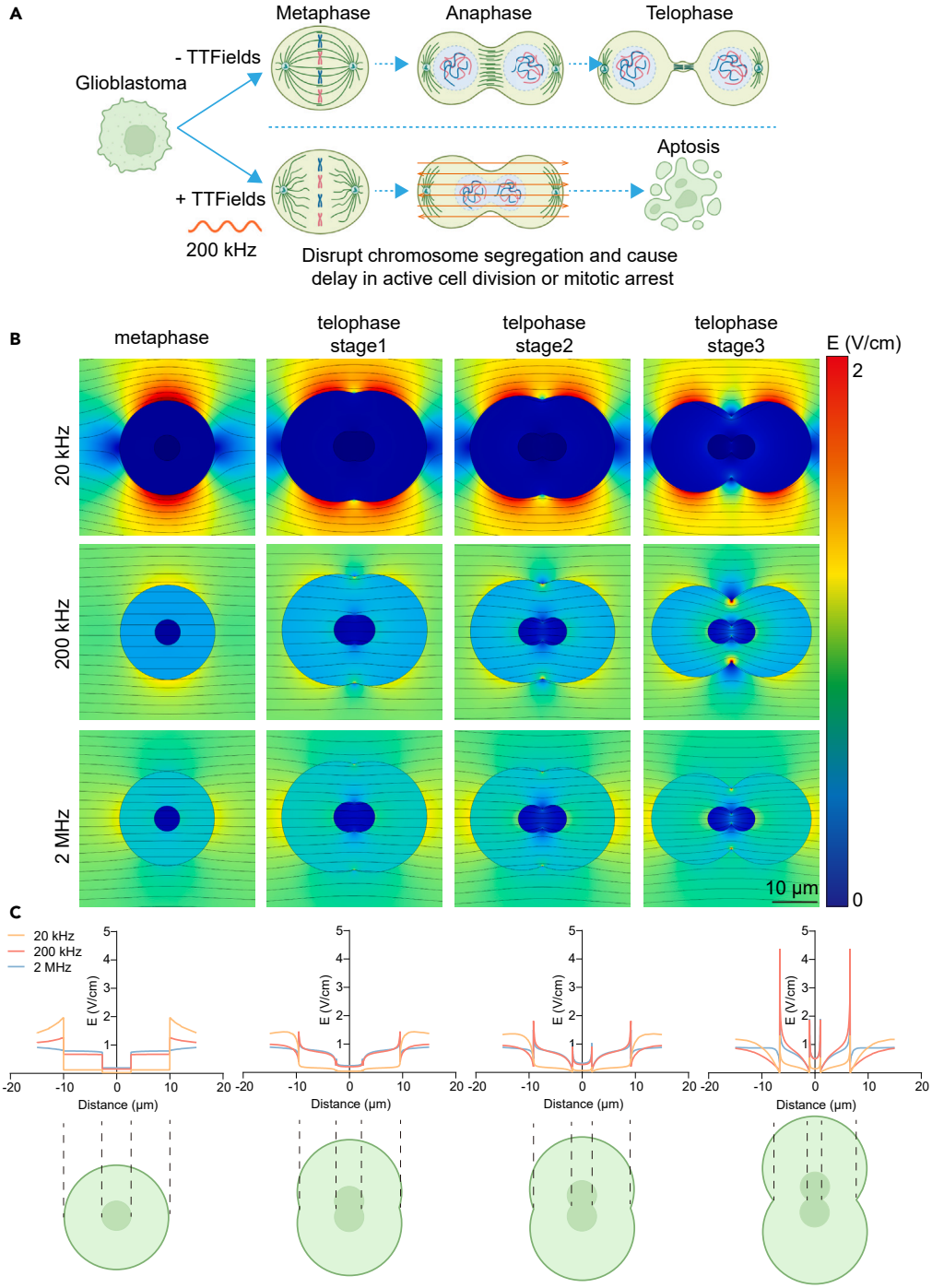

Figure 1. Electromagnetic effect simulation

(A) Mechanism of action of TTFields. TTFields disrupt mitosis of glioblastoma or other rapidly dividing cells, leading to apoptosis (programmed cell death).

(B) Simulation of electric field distribution by application of a homogeneous electrical field (1 V/cm) with different frequencies on mitosis. Scale bar, 10 μm.

(C) Quantification of electric field distribution through the cell on the central axis by application of a homogeneous electrical field (1 V/cm) with different frequencies on mitosis.

quantified the cell division cycle and found that IF had the greatest effect on the cell division cycle over these three frequencies, preventing cells from continuing to divide, whereas low and radio frequency stimulation prolonged the cell cycle, but the cells were eventually able to complete cell division (Figure 2B). To quantitatively measure TTFields' effects on cell proliferation inhibition, cell number was counting after termination of 24 h TTFields treatment (Figure 2C). Compared with the untreated group, cell proliferation capacity decreased by 54% and 46%

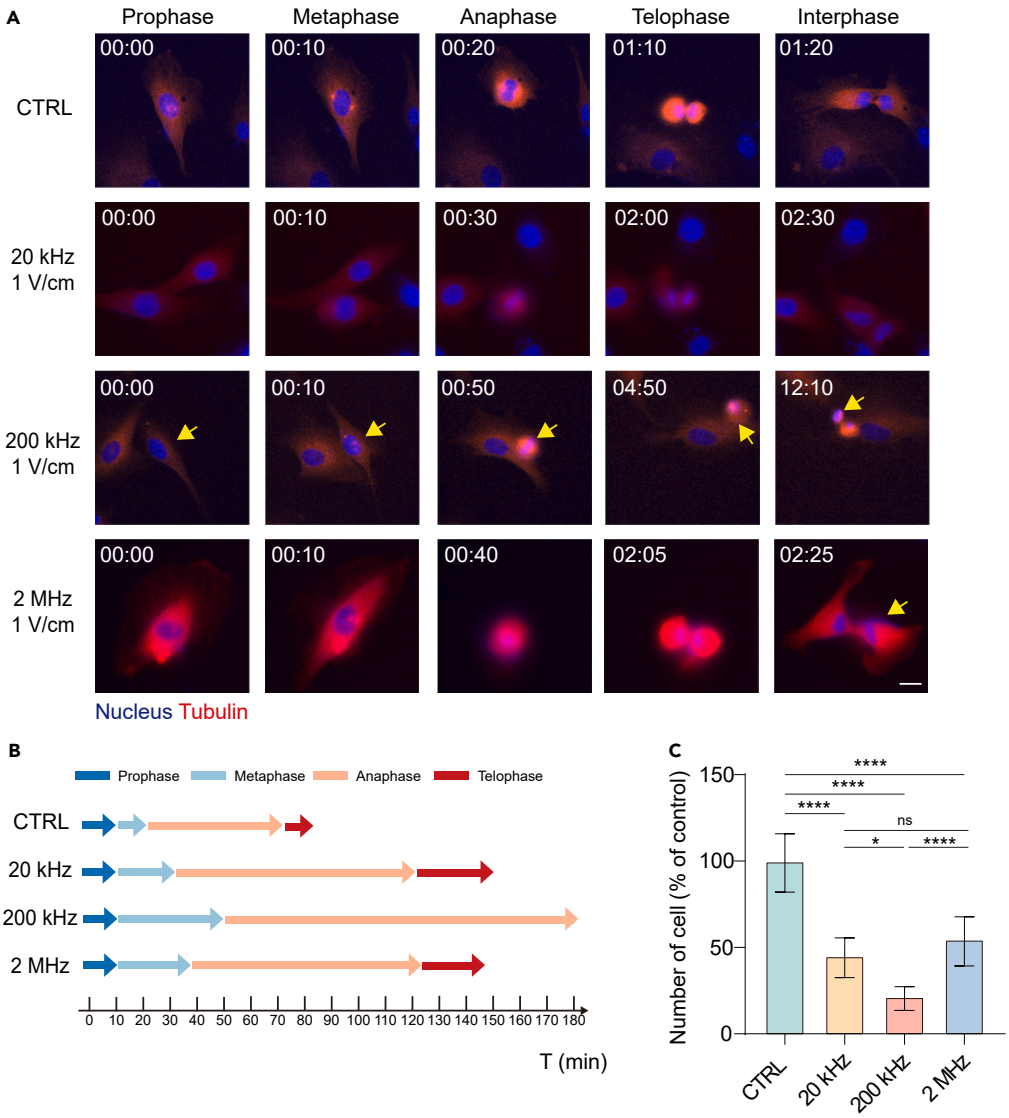

Figure 2. TTFields inhibit gliomas mitosis

(A) Representative time-lapse images showing the U87-MG cells expressing tubulin (red) and nucleus (blue) with and without different frequencies (20 kHz, 200 kHz, and 2 MHz) and low-intensity electric fields at 1 V/cm. Abnormal division of the cell nucleus (yellow arrow). Scale bar, 20 μm.

(B) Timeline showing mitotic period of U87-MG cells with and without different frequencies (20 kHz, 200 kHz, and 2 MHz) electric field, including prophase, metaphase, anaphase, and telophase.

(C) Graph showing cell viability after 24-h electrical stimulation. Results are expressed as mean ± standard deviation with 95% CI (n = 10). Statistically significant results are shown as ns = 0.6835, *p < 0.05, ****p < 0.0001.

after LF and RF AC stimulation, respectively, and IF had the highest inhibition rate of cell proliferation capacity, reaching 78%. Similar results were found in a previous report that IF significantly suppressed GBM propagation. However, no explanation was given for the non-selection of low and radio frequencies.[13,14] Taken together, both simulated and experimental data verified that the strongest electric field strength by cells can be achieved with IF stimulation, resulting in a higher inhibition of cell proliferation.

Effects of TTFields in cell migration inhibition

Highly invasive cell growth is a hallmark of malignancy in GBM and is one of the factors that contribute to the aggressive behavior of this type of brain tumor.[15] The invasive nature of GBM cells makes it difficult to treat. Currently, TTFields have been validated to inhibit tumor cell migration and invasion. Previous research has demonstrated that TTFields hinder Septin association with microtubules during cell attachment and spreading to fibronectin.[16,17] Microtubules are also known to regulate movement and key signaling events.[18] Although, it remains unclear whether the efficacy is frequency-dependent.[7] Therefore, we performed a cell migration study and measured the change in diffusion

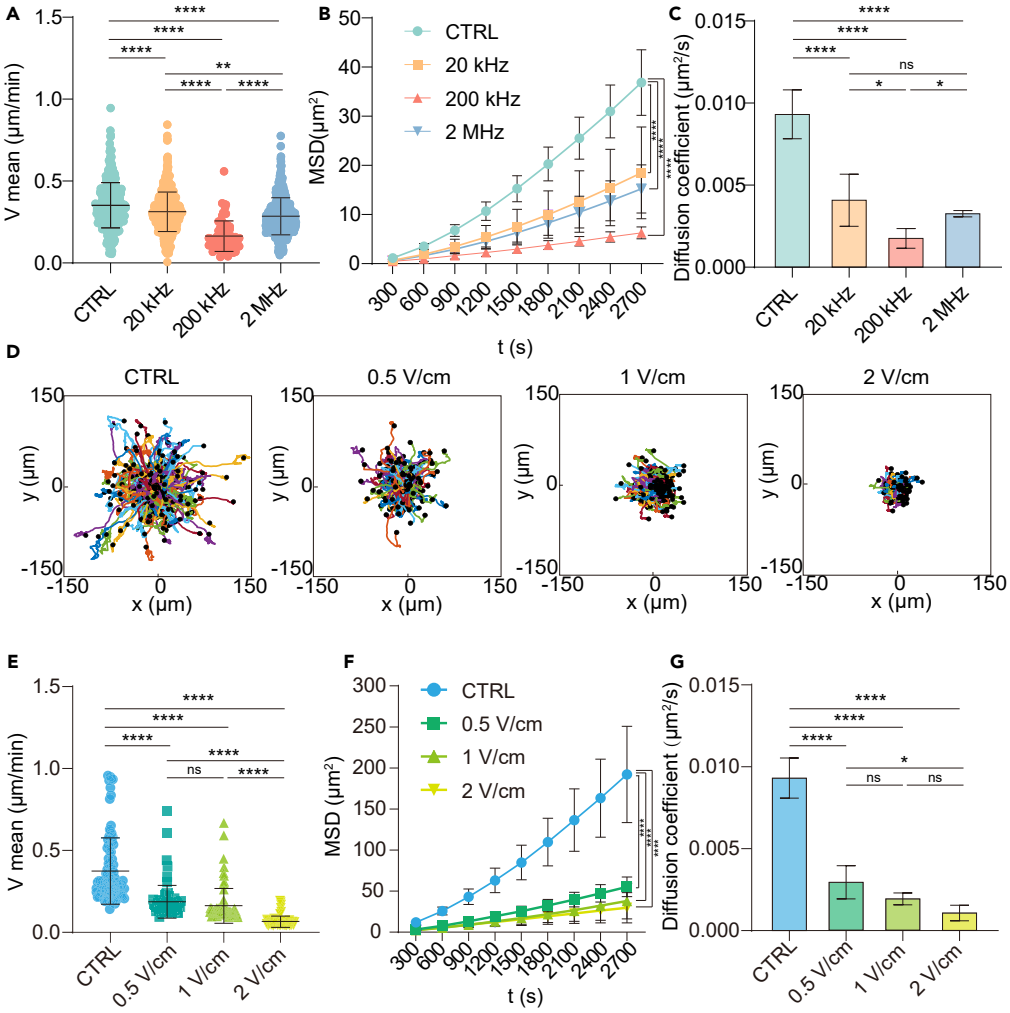

Figure 3. TTFields hinder gliomas migration capacity

(A–C) Comparison of migration parameters for U87-MG cells under different frequencies electric field (20 kHz, 200 kHz, and 2 MHz, at 1 V/cm) and control of directional migration: (A) mean migration velocity, (B) mean square displacement (MSD), and (C) diffusion coefficient. Results are expressed as mean ± standard error of the mean with 95% CI (for MSD and diffusion coefficient, n = 5, for mean migration velocity n_{CTRL} = 350 cells, $n_{20\ kHz}$ = 435 cells, $n_{200\ kHz}$ = 320 cells, $n_{2\ MHz}$ = 400 cells); *p < 0.05, **p < 0.01, ****p < 0.0001, ns = 0.1939 by one-way *ANOVA* for multiple comparisons.

(D–G) Comparison of migration parameters for U87-MG cells under different intensity electric field (0.5 V/cm, 1 V/cm, and 2 V/cm, at 200 kHz) and control of directional migration: (D) cell migration trajectories, (E) mean migration velocity, (F) mean square displacement (MSD), and (G) diffusion coefficient. Results are expressed as mean ± standard error of the mean with 95% CI (for MSD and diffusion coefficient, n = 5, for mean migration velocity n_{CTRL} = 95 cells, $n_{0.5\ V/cm}$ = 75 cells, $n_{1\ V/cm}$ = 74 cells, $n_{2\ V/cm}$ = 75 cells); *p < 0.05, **p < 0.01, ****p < 0.0001 by one-way *ANOVA* for multiple comparisons.

coefficient, persistence, and migration speed at different frequencies to characterize the changes in migration capacity (Video S1). After continuous tracking of each cell migration, the statistical analysis results showed that the diffusion of coefficient of U87-MG cells significantly decreased after different frequency AC stimulation, especially in the IF group compared with the untreated group, which decreased by 80% (Figure 3A). The mean square displacement (MSD) is a useful measure to find cell persistence of migration in two- and three-dimension microenvironments.[19] The MSD and migration speed results showed that the persistence of U87-MG migration similarly decreased, and trend was the same as the previous diffusion coefficient (Figures 3B and 3C). The migration of invasive cancer cell such as U87-MG is in the form of mesenchymal cell migration, which is a motility mode characterized by cell polarization to form a leading edge that extends actin-rich protrusions.[20] Thus, cell membrane produces a depression during migration similar to cleavage furrow region in mitosis, and thus, this region also absorbs energy affecting microtubule aggregation and interfering with migration. The hypothesis that electromagnetic forces damage microtubules is based on the fact that the tubulin dimer, which is the fundamental component of microtubules, possesses a significant electric dipole moment.[21] Consequently, the dipole moment induced by TTField forces on charged dimers may influence dimer orientation, resulting in a failure of microtubule assembly and interference with mitotic progression, as well as weakening cell migration ability. It has been proposed that TTFields' inhibition of cell migration is dependent on frequency, intensity, duration, and direction.[22] In short, these results

demonstrated that IF stimulation could largely reduce cell migration capacity, which is correlated with the highest energy uptake by cells during IF stimulation.

With respect to the frequency, the cell migration studies reveal a frequency-dependent efficiency of the TTFields. To further investigate whether the effect of inhibition of cell migration is field-strength-dependent, we performed stimulation with different electric field strengths using an AC electric field of the same frequency (200 kHz) (Video S2). We tracked individual cell trajectories for 24 h to investigate the influence of migration behavior of U87-MG after different electric field strength AC stimulation (Figure 3D). Based on the analysis of the migration trajectory, the migration distance of cells decreased with increasing electric field strength. Meanwhile, the cell migratory capacity of cells has the same trend in coefficient, persistence, and migration speed (Figures 3E, 3F, and 3G). Taken together, the variation in electric field distribution caused by different frequencies and amplitudes of AC stimulation results in varying degrees of microtubule polymerization. These results demonstrated that the migration ability of U87-MG cells was inhibited by TTFields and was frequency- and field-strength-dependent, which has the potential to guide the optimization of parameters for clinical treatment. By understanding this mechanism, TTFields can be applied to more cancers in the future.

DISCUSSION

Currently, the mechanism of action of TTFields is thought to involve hindering the formation of microtubules by applying an electric field of specific intensity, thereby disrupting the functional integrity of the spindle.[23] However, there remains a notable discrepancy between the attributes of the electric field, such as amplitude and frequency, and the actual termination of cellular division, lacking clear supporting evidence. In this study, we aim to establish a connection between the cessation of cellular division induced by high-frequency electric field . Previous investigations have thoroughly examined the physical effects of cellular exposure to radiofrequency electromagnetic fields, suggesting that the cell cleavage furrow experiences heightened electric intensities.[7] Nevertheless, it is important to note that high electric field strength alone does not directly indicate reduced cell mitosis.

To address these gaps in knowledge, our study begins by elucidating the electromagnetic field model across a broader frequency domain than previously explored, specifically focusing on the application scope of TTFields. In contrast to earlier models, we incorporate a dual-dielectric model to depict the electric environment that the cellular nucleus experiences under the influence of high-frequency electric terrains. Our findings demonstrate that intermediate-frequency electrotherapy leads to a substantial 246% increase in electric field strength at the cleavage furrow region during cell division, compared with metaphase, suggesting a stronger electric field force. In contrast, low-frequency electrotherapy results in a 32% decrease, whereas high-frequency electrotherapy leads to a significant 198% increase in electric field strength. This implies that high-frequency alternating electric fields also affect the negatively charged DNA within the nucleus. The analytical outcomes obtained from our proposed model provide robust evidence, aligning with observations of DNA replication reduction and hindered repair of double-helix DNA breaks when cells are exposed to TTFields, as detailed by Karanam et al.[24]

Additionally, empirical observations within the defined frequency limits reveal the resilience of cell mitosis to a 20 kHz AC electric current, indicating its inability to penetrate the cell membrane. Our data suggest that optimizing TTFields in preclinical models could affect the proliferation and migration behavior of cells associated with electric field enhancement. Specifically, under the stimulation of 200 kHz, the cell proliferation rate decreased by 78%, and the directed cell migration rate decreased by 54%. Moreover, as the electric field intensity increased, the inhibitory effect on cell migration increased from 46% to 89%. Interestingly, with even greater frequency amplification, cellular propagation resurges, suggesting that thorough infiltration of the electric field into the nucleus ultimately diminishes its influence within the cytosol, attaining maximum force exertion on the nuclear membrane. This inherent dynamic trajectory suggests that the primary influence of TTFields on cellular division predominantly affects the cellular cytosol. Our results are consistent with predictions made by Tuszynski et al. through equivalent circuit modeling.[25]

Consequently, our findings suggest that the main role of TTFields is to direct the electric field within the cytoplasm. As the frequency of the applied electric field increases, it initially penetrates the cell membrane, gradually intensifying the electric strength experienced by the cytoplasm. This potent dielectrophoretic force restricts the movement of microtubules, inhibiting the formation of the spindle apparatus. As the frequency further rises, the applied field permeates the nuclear envelope, resulting in reduced electric strength in the cytoplasm and subsequent attenuation of the electrostatic force that inhibits microscopic migration. However, the electric force within the cell nucleus hampers essential biological functions, such as DNA repair, thereby enhancing the electric field's lethal effect on cancerous cells. Therefore, our research suggests that labeling microtubules may serve as a clearer indicator for determining the applicable range within the TTF frequency domain. Furthermore, understanding the intracellular signaling pathways associated with TTF will be prioritized in future investigations.

Limitations of the study

Combining numerical simulation and experimental verification helped shed light on the frequency-dependent and field-strength-dependent effects on cell mitosis by TTFileds. We could not figure out at which specific stage during cell mitosis that TTFields commence the block of cell division. Albeit we have demonstrated TTFields disrupted the separation of chromosome during cell mitosis, the distribution of electric stress imposed on glioblastoma cells has not been directly obtained by virtue of experimental methods. In the future, biomechanical and cytomic information from traction force microscopy and omics techniques will further deepen the understanding of the mechanism of TTField's effects on cell mitosis.

STAR★METHODS

Detailed methods are provided in the online version of this paper and include the following:

- KEY RESOURCES TABLE
- RESOURCE AVAILABILITY
  - Lead contact
  - Materials availability
  - Data and code availability
- EXPERIMENTAL MODEL AND STUDY PARTICIPANT DETAILS
  - Cell culture and cell transfection
- METHOD DETAILS
  - Tumor treating fields
  - Live-cell imaging
  - Cell migration
  - Cell counting
  - Finite element mesh simulations
- QUANTIFICATION AND STATISTICAL ANALYSIS

SUPPLEMENTAL INFORMATION

Supplemental information can be found online at https://doi.org/10.1016/j.isci.2023.108575.

ACKNOWLEDGMENTS

This study was supported by grants from the Pioneering Project of Academy for Engineering and Technology of Fudan University, China (No. gyy2018-002) and the National Natural Science Foundation of China (Nos. 22274026, 31870978, 51877046).

AUTHOR CONTRIBUTIONS

Conception and design of research: X-W. X., H-T. L., and K-F. L. Conception and design of the experiments: X-W. X., H-T. L., X-N. T., Y-J. L., and K-F. L. Collection, analysis, and interpretation of data: X-W. X., H-T. L., X-N. T., Y-L. Z., and J. L. Drafting the article or revising it critically for important intellectual content: X-W. X., H-T. L., X-N. T., Y-L. Z., C.W., S-X. Y., H. Z., Y-J. L., and K-F. L. All authors approved the final version of the manuscript and listed qualify for authorship.

DECLARATION OF INTERESTS

The authors declare no competing interests.

Received: June 4, 2023
Revised: October 6, 2023
Accepted: November 21, 2023
Published: November 23, 2023

REFERENCES

1. Makovec, T. (2019). Cisplatin and beyond: molecular mechanisms of action and drug resistance development in cancer chemotherapy. Radiol. Oncol. *53*, 148–158.
2. Qiu, Z., Yu, Z., Xu, T., Wang, L., Meng, N., Jin, H., and Xu, B. (2022). Novel Nano-Drug Delivery System for Brain Tumor Treatment. Cells *11*, 3761.
3. Fonkem, E., and Wong, E.T. (2012). NovoTTF-100A: a new treatment modality for recurrent glioblastoma. Expert Rev. Neurother. *12*, 895–899.
4. Leal, T., Kotecha, R., Ramlau, R., Zhang, L., Milanowski, J., Cobo, M., Roubec, J., Petruzelka, L., Havel, L., Kalmadi, S., et al. (2023). Tumor Treating Fields therapy with standard systemic therapy versus standard systemic therapy alone in metastatic non-small-cell lung cancer following progression on or after platinum-based therapy (LUNAR): a randomised, open-label, pivotal phase 3 study. Lancet Oncol. *24*, 1002–1017.
5. Yang, Y., Hu, X., Liu, Y., Ouyang, B., Zhang, J., Jin, H., Yu, Z., Liu, R., Li, Z., Jiang, L., et al. (2022). An implantable ultrasound-powered device for the treatment of brain cancer using electromagnetic fields. Sci. Adv. *8*, eabm5023.
6. Kirson, E.D., Gurvich, Z., Schneiderman, R., Dekel, E., Itzhaki, A., Wasserman, Y., Schatzberger, R., and Palti, Y. (2004). Disruption of cancer cell replication by alternating electric fields. Cancer Res. *64*, 3288–3295.
7. Kirson, E.D., Dbalý, V., Tovaryš, F., Vymazal, J., Soustiel, J.F., Itzhaki, A., Mordechovich, D., Steinberg-Shapira, S., Gurvich, Z., Schneiderman, R., et al. (2007). Alternating electric fields arrest cell proliferation in animal tumor models and human brain tumors. Proc. Natl. Acad. Sci. USA *104*, 10152–10157.
8. Davies, A.M., Weinberg, U., and Palti, Y. (2013). Tumor treating fields: a new frontier in cancer therapy. Ann. N. Y. Acad. Sci. *1291*, 86–95.
9. Challis, L.J. (2005). Mechanisms for interaction between RF fields and biological tissue. Bioelectromagnetics *26*, S98–S106.
10. Berkelmann, L., Bader, A., Meshksar, S., Dierks, A., Hatipoglu Majernik, G., Krauss, J.K., Schwabe, K., Manteuffel, D., and Ngezahayo, A. (2019). Tumour-treating fields (TTFields): Investigations on the mechanism of action by electromagnetic exposure of cells in telophase/cytokinesis. Sci. Rep. *9*, 7362.
11. Wong, E.T., Lok, E., and Swanson, K.D. (2018). Alternating electric fields therapy for malignant gliomas: from bench observation

to clinical reality. Prog. Neurol. Surg. *32*, 180–195.

12. Spiliotis, E.T., Kinoshita, M., and Nelson, W.J. (2005). A mitotic septin scaffold required for Mammalian chromosome congression and segregation. Science *307*, 1781–1785.
13. Kim, E.H., Song, H.S., Yoo, S.H., and Yoon, M. (2016). Tumor treating fields inhibit glioblastoma cell migration, invasion and angiogenesis. Oncotarget *7*, 65125–65136.
14. Neuhaus, E., Zirjacks, L., Ganser, K., Klumpp, L., Schüler, U., Zips, D., Eckert, F., and Huber, S.M. (2019). Alternating electric fields (TTFields) activate Cav1. 2 channels in human glioblastoma cells. Cancers *11*, 110.
15. Wong, E.T., Hess, K.R., Gleason, M.J., Jaeckle, K.A., Kyritsis, A.P., Prados, M.D., Levin, V.A., and Yung, W.K. (1999). Outcomes and prognostic factors in recurrent glioma patients enrolled onto phase II clinical trials. J. Clin. Oncol. *17*, 2572–2578.
16. Gera, N., Yang, A., Holtzman, T.S., Lee, S.X., Wong, E.T., and Swanson, K.D. (2015). Tumor treating fields perturb the localization of septins and cause aberrant mitotic exit. PLoS One *10*, e0125269.
17. Moser, J.C., Salvador, E., Deniz, K., Swanson, K., Tuszynski, J., Carlson, K.W., Karanam, N.K., Patel, C.B., Story, M., Lou, E., and Hagemann, C. (2022). The mechanisms of action of Tumor Treating Fields. Cancer Res. *82*, 3650–3658.
18. Garcin, C., and Straube, A. (2019). Microtubules in cell migration. Essays Biochem. *63*, 509–520.
19. Stokes, C.L., Lauffenburger, D.A., and Williams, S.K. (1991). Migration of individual microvessel endothelial cells: stochastic model and parameter measurement. J. Cell Sci. *99*, 419–430.
20. Sanz-Moreno, V., Gadea, G., Ahn, J., Paterson, H., Marra, P., Pinner, S., Sahai, E., and Marshall, C.J. (2008). Rac activation and inactivation control plasticity of tumor cell movement. Cell *135*, 510–523.
21. Tuszynski, J., Luchko, T., Carpenter, E., and Crawford, E. (2004). Results of molecular dynamics computations of the structural and electrostatic properties of tubulin and their consequences for microtubules. J. Comput. Theor. Nanosci. *1*, 392–397.
22. Tanzhu, G., Chen, L., Xiao, G., Shi, W., Peng, H., Chen, D., and Zhou, R. (2022). The schemes, mechanisms and molecular pathway changes of Tumor Treating Fields (TTFields) alone or in combination with radiotherapy and chemotherapy. Cell Death Discov. *8*, 416.
23. Wenger, C., Salvador, R., Basser, P.J., and Miranda, P.C. (2015). The electric field distribution in the brain during TTFields therapy and its dependence on tissue dielectric properties and anatomy: a computational study. Phys. Med. Biol. *60*, 7339–7357.
24. Karanam, N.K., Ding, L., Aroumougame, A., and Story, M.D. (2020). Tumor treating fields cause replication stress and interfere with DNA replication fork maintenance: implications for cancer therapy. Transl. Res. *217*, 33–46.
25. Tuszynski, J.A., Wenger, C., Friesen, D.E., and Preto, J. (2016). An overview of sub-cellular mechanisms involved in the action of TTFields. Int. J. Environ. Res. Public Health *13*, 1128.
26. Wang, K., Xie, S., Ren, Y., Xia, H., Zhang, X., and He, J. (2012). Establishment of a bioluminescent MDA-MB-231 cell line for human triple-negative breast cancer research. Oncol. Rep. *27*, 1981–1989.
27. Schindelin, J., Arganda-Carreras, I., Frise, E., Kaynig, V., Longair, M., Pietzsch, T., Preibisch, S., Rueden, C., Saalfeld, S., Schmid, B., et al. (2012). Fiji: an open-source platform for biological-image analysis. Nat. Methods *9*, 676–682.
28. Tinevez, J.Y., Perry, N., Schindelin, J., Hoopes, G.M., Reynolds, G.D., Laplantine, E., Bednarek, S.Y., Shorte, S.L., and Eliceiri, K.W. (2017). TrackMate: An open and extensible platform for single-particle tracking. Methods *115*, 80–90.
29. Gorelik, R., and Gautreau, A. (2014). Quantitative and unbiased analysis of directional persistence in cell migration. Nat. Protoc. *9*, 1931–1943.
30. Friedl, P., Sahai, E., Weiss, S., and Yamada, K.M. (2012). New dimensions in cell migration. Nat. Rev. Mol. Cell Biol. *13*, 743–747.
31. Chang, S.S., Guo, W.H., Kim, Y., and Wang, Y.L. (2013). Guidance of cell migration by substrate dimension. Biophys. J. *104*, 313–321.
32. Wu, P.-H., Giri, A., Sun, S.X., and Wirtz, D. (2014). Three-dimensional cell migration does not follow a random walk. Proc. Natl. Acad. Sci. USA *111*, 3949–3954.
33. Yu, S.-X., Liu, Y., Wu, Y., Luo, H., Huang, R., Wang, Y.-J., Wang, X., Gao, H., Shi, H., Jing, G., and Liu, Y.J. (2022). Cervix chip mimicking cervical microenvironment for quantifying sperm locomotion. Biosens. Bioelectron. *204*, 114040.
34. DeBruin, K.A., and Krassowska, W. (1999). Modeling electroporation in a single cell. I. Effects of field strength and rest potential. Biophys. J. *77*, 1213–1224.
35. Krassowska, W., and Filev, P.D. (2007). Modeling electroporation in a single cell. Biophys. J. *92*, 404–417.

STAR★METHODS

KEY RESOURCES TABLE

REAGENT or RESOURCE	SOURCE	IDENTIFIER
Bacterial and virus strains		
lentiviral vectors pLV-Tubulin-mCherry	Inovogen Tech. Co.	Cat #VL3509
Chemicals, peptides, and recombinant proteins		
FBS	Gibco	Cat #10099141C
DMEM	Gibco	Cat #11960044
penicillin/streptavidin	Thermo	Cat #15140122
Hoechst 33258 dye	Sigma	Cat #94403
Fibronectin	Sigma	Cat #F0895
Experimental models: Cell lines		
U87-MG	NCACC	N/A
U87-MG-tubulin	This paper	N/A
Software and algorithms		
ImageJ	Schneider et al.	https://ImageJ.nih.gov/ij/
MATLAB	MathWorks	https://www.mathworks.com/products/matlab.html
COMSOL 5.4 Multiphysics	Stockholm	https://cn.comsol.com/
GraphPad Prism 9	Graphpad Software	https://www.graphpad.com
Customized MATLAB scripts	Previously published	https://doi.org/10.1016/j.bios.2022.114040
Device		
Arbitrary waveform function generator	RIGOL	Cat #CZ3457
Inverted fluorescence microscope	Leica	Cat #DMi8

RESOURCE AVAILABILITY

Lead contact

Lead Contact Requests regarding reagents and resource sharing will be addressed by the lead contact, Dr. Ke-Fu Liu (kfliu@fudan.edu.cn).

Materials availability

This study did not generate new unique reagents.

Data and code availability

(1) Original data reported in this paper will be provided upon request by the lead contact.
(2) This paper reports no original code.
(3) Any additional information required to reanalyze the data reported in the paper is available from the lead contact upon request.

EXPERIMENTAL MODEL AND STUDY PARTICIPANT DETAILS

Cell culture and cell transfection

U87-MG cells were purchased from National Collection of Authenticated Cell Cultures (NCACC, China). U87-MG cells expressing the tubulin (U87-MG-tubulin) were obtained after retroviral transduction and maintained in culture according to a previously described protocol.[26] These cells lines were grown in DMEM medium supplemented with 10% (v/v) fetal bovine serum (Gibco, USA) and penicillin/streptavidin (final concentration 50 μg/mL; Thermo, USA), and incubated at 37°C, 5% CO_2 atmosphere.

METHOD DETAILS

Tumor treating fields

The arbitrary waveform function generator (RIGOL, China) was used to generate low-intensity electric fields at the desired frequencies in the medium, two pairs of perpendicular gold electrodes placed parallel to each other with a diameter of about 10 mm in the middle of a Petri dish. So that cells were seeded in the middle of the well, and after 24h TTFields were started with different voltage and frequency. Plate temperature was maintained 37°C and supplied with 5% CO_2. Duration of TTFields exposure lasted anywhere from 24 h.

Live-cell imaging

For long-term live cell mitosis and migration imaging, we used genetically modified U87-MG cells whereby the glioblastoma cells were transfected with lentiviral vectors that expressed tubulin-mCherry. Cells were plated on fibronectin (25 μg/mL)-coated glass-bottom cell culture dishes and maintained in complete culture medium without penicillin and streptomycin at 37°C throughout the imaging process. For nuclei staining, Hoechst 33258 dye (Sigma, USA) was added to complete culture medium at a final concentration of 1 μg/mL, and cells were incubated at 37°C for 30 min before the acquisition of images. Time-lapse imaging was recorded using an inverted fluorescence microscope (DMi8, Leica).

Cell migration

In order to quantify the cell migration, we tracked the cells in time-lapse imaging. The dynamic images were analyzed by the Trackmate plugin in FIJI ImageJ to obtain the cell tracking information.[27,28] Cell tracks were filtered to only keep those with good fidelity, as measured through Trackmate's 'quality' filter. Mean squared displacement (MSD) is a common metric for measuring migration speed and distance traveled, which can be used to characterize cell persistence.[29,30] The MSD is given by:

$$MSD(\tau) = nS^2P^2\left(e^{-\frac{\tau}{P}} + \frac{\tau}{P} - 1\right) \quad \text{(Equation 1)}$$

where P is the persistent time, S is the cell speed, n is the dimension of the extracellular space (which can be 1D, 2D, and 3D),[31] and τ is the time lag between positions of the cell. The autocorrelation function of the cell velocity vector for the classical persistent random walk (PRW) model of cell migration exhibits a single exponential decay:

$$< v(\tau)v(0) > = \frac{nD}{P}e^{-\frac{\tau}{P}} \quad \text{(Equation 2)}$$

where D is the cell diffusivity. In the 2D, the velocity direction is described by an angle with respect to a laboratory frame, θ. The change in angle over a small-time interval, $d\theta$, is a random variable given by a uniform distribution with a peak near $d\theta = 0$. Typically, Equation 1 was used to fit measured MSD data. The statistics of $d\theta$ and the time lag dependence of the velocity autocorrelation function (Equation 2) are generally not examined in detail.[32] A customized MATLAB (MathWorks, Natick, MA) script was used to analyze the trajectories, velocities, diffusion coefficients, and migration angles.[33]

Cell counting

In order to identify the inhibition of cell growth after different TTFields treatment, we analyzed it by quantifying the cell count. The relative number of live cells at the end of treatment was expressed as a percentage of untreated control cells. The inhibition rate was calculated based on the following equations:

$$Inhibition\ rate\ (\%control) = \frac{The\ number\ of\ live\ cells\ in\ treatment}{The\ number\ of\ live\ cells\ in\ control\ group} \times 100\% \quad \text{(Equation 3)}$$

Finite element mesh simulations

The finite element method (FEM) is a commonly used technique for calculating the electric field distribution in complex geometries such as the cell. Given that TTFields has been reported to have an effect on mitotic cells, we chose to examine this phenomenon in the context of mitotic cells, which display a highly spherical geometry. The numerical simulation used to qualitatively verify the electric potential distributions on individual cells and monolayers cells subjected to the same uniform electric field was performed in COMSOL 5.4 Multiphysics (Stockholm, Sweden). A simple two-dimensional geometry, consisting of three 20 μm diameter circles placed in the center, was used to model the simplified equivalent circuit. In order to distinguish the different stages of telophase, we adjusted the distances between the cytoplasm and nucleoplasm, where the cytoplasm was 6, 8 and 15 μm, representing stage 1, 2 and 3, respectively, while the distance between the nucleoplasm was 2, 4 and 5 μm, respectively. Electric potential φ can be solved according to the following equation:

$$\nabla \bullet \left(\left(\sigma + \varepsilon\frac{\partial}{\partial t}\right)\nabla\varphi(x, y, t)\right) = 0 \quad \text{(Equation 4)}$$

where σ is conductivity, and ε is the relative permittivity. This equation describes the electric potential $\varphi(x, y, t)$ as a function of the distribution of space and time. The conductivity of the suspension is 0.2 S/m, the conductivity of the cell is 0.3 S/m, the relative permittivity of the suspension is 80, and the relative permittivity of the cell is 154.4. These parameters designed in the model were based on previous studies.[34,35]

We simplified the equation for the steady state ($\frac{\partial}{\partial t} = 0$) and uniform conductivity ($\nabla \bullet \sigma = 0$), and then we obtained the Laplace's equation.

$$\nabla \bullet \nabla\varphi(x, y) = 0. \quad \text{(Equation 5)}$$

The electric field strength is the gradient of the electric potential, so

$$E = -\nabla\varphi \quad \text{(Equation 6)}$$

The left wall (x = 0) was provided with voltage while the right wall was grounded, and the top and bottom borders were defined as an insulating boundary.

QUANTIFICATION AND STATISTICAL ANALYSIS

Unless stated otherwise, data are expressed as mean ± SE. Multiple comparisons were analyzed by a one-way ANOVA, and differences in the mean values among groups were conducted by a Dunnett post-hoc correction. All experiments were repeated at least three times. *p < 0.05, **p < 0.01, ***p < 0.001, ****p < 0.0001 were considered statistically significant.